FEBS Letters 581 (2007) 4120–4124

The protonation state of the catalytic aspartates in plasmepsin II

Ran Friedman*, Amedeo Caflisch*

Department of Biochemistry, University of Zürich, Winterthurerstrasse 190, CH-8057 Zürich, Switzerland

Received 3 May 2007; revised 12 July 2007; accepted 13 July 2007

Available online 25 July 2007

Edited by Peter Brzezinski

Abstract **Assigning the correct protonation state to the catalytic residues is essential for a realistic modelling of an enzyme's active site. Plasmepsins are pharmaceutically relevant aspartic proteases involved in haemoglobin degradation by *Plasmodium* spp. In aspartic proteases, one of the two catalytic aspartates is protonated, while the other is negatively charged. Here, multiple explicit-water molecular dynamics simulations of plasmepsin II, uncomplexed and with a hydroxypropylamine peptidomimetic inhibitor, indicate that protonation of Asp214 favours a stable active site structure. Moreover, the protonation state of the catalytic aspartate has a strong influence on a linear chain of hydrogen bonds with the adjacent side chains.**

Keywords: Malaria; Aspartic protease; Plasmepsin; Proplasmepsin; Molecular dynamics; Protonation

1. Introduction

The malaria parasite, *Plasmodium*, digests host haemoglobin as a nutritional source during the erythrocytic stage of the disease. Four pepsin-like aspartic proteases, named plasmepsins (PM I–IV), are involved in haemoglobin breakdown in *Plasmodium falciparum*, which causes the most fatal form of malaria. As PMs are unique to Plasmodia, these enzymes are regarded as potential drug targets [1]. However, despite their pharmaceutical significance, the dynamics of PMs have only recently started to be investigated by computational studies [2–5]. Conversely, the folding and ligand binding of an AIDS related retroviral aspartic protease, HIV protease, were studied by different simulation techniques, including implicit and explicit solvent molecular dynamics (MD), Brownian dynamics and Gō models (see e.g. [6–8]).

PM II is the most studied PM. It is translated as an inactive zymogen (proenzyme), and its activation involves the cleavage of its N-terminal part. This transition (maturation) brings about a domain shift in the enzyme's N-domain [9], which enables the formation of the catalytic site. The catalytic residues are D34 and D214, one of which is protonated while the other is negatively charged in the digestive vacuole (pH $\approx$ 5) where haemoglobin cleavage takes place.

Simulation and docking studies of aspartic proteases have shown that assigning the correct protonation state to the catalytic residues is necessary for a realistic modelling of the binding site. This is particularly relevant in computer-aided drug design, where the calculated binding energies are often sensitive to the location of protons in the binding site. Accordingly, this problem has been addressed, e.g., in β-secretase (BACE), but despite efforts from several groups [10–13] there is yet no consensus regarding the protonation state. Similarly, the protonation state of the catalytic aspartates in PM II is not known. In a very interesting computational study of the catalytic mechanism in PM II, D34 was protonated [3], but protonation of D214 was observed to yield a better agreement with the binding energies of specific PM IV inhibitors [14].

Here, the protonation state of the catalytic aspartates in PM II is investigated by explicit solvent molecular dynamics (MD) simulations. The results of 22 independent MD runs, for a total simulation time of more than 0.45 μs are reported below. Four MD runs of PM II were started from the crystal structure of the apo enzyme (PDB: 1LF4 [15]). In two of these runs, D34 was protonated and D214 was negatively charged, while in the remaining two D214 was protonated and D34 was negatively charged. Six runs, three with D34 protonated and three with D214 protonated were started from the proPM structure (PDB: 1PFZ [9]) upon manual removal of the N-terminal prosegment. The simulations of cleaved proPM were performed to examine the effect of protonation state on the maturation of the enzyme (structural details on the conformational transitions involved in the maturation process will be given elsewhere). Four additional runs were performed using a structure of PM II with an alternative conformation of the flap region (PDB:2BJU [16]). Finally, eight simulations of PM II in the presence of a transition state analogue inhibitor, were carried out to examine the protonation state of the complexed enzyme. The analysis of the simulations shows that the protonation of D214 favours a stable active site structure, which is consistent with the crystal structures of the protein. Moreover, it is shown that the choice of protonation state influences the stability of the chain of hydrogen bonds at the catalytic site.

2. Methods

2.1. Molecular dynamics simulations

MD simulations were performed by use of the Gromacs program [17,18], version 3.3.1, with the OPLS-AA force field [19]. Simulations of mature PM II were carried out using the structure of the apo-enzyme (PDB:1LF4 [15]). Five loop residues were not located in the experiment (residues 238–243) and were modelled based on a structure

*Corresponding authors. Fax: +41 44 635 68 62.
E-mail addresses: r.friedman@bioc.uzh.ch (R. Friedman), caflisch@bioc.uzh.ch (A. Caflisch).

Abbreviations: PM, plasmepsin; MD, molecular dynamics; BACE, β-secretase; PDB, protein data bank; RMSD, root mean square deviation; HB, hydrogen bond

0014-5793/$32.00
doi:10.1016/j.febslet.2007.07.033

of PM II complexed with pepstatin (PDB:1XE5). The structure of the proenzyme (PDB:1PFZ [9]) was used for simulations of the cleaved zymogen. All residues belonging to the premature portion of the enzyme were deleted, to obtain a model structure of the enzyme immediately after the cleavage of its premature segment. Missing residues at the flap region were assumed to have an open conformation, since it allows more conformational freedom [20]. They were therefore modelled based on the structure of PM II with an open flap conformation (PDB:2BJU [16]). The same structure was also used to simulate the protein in the alternative (open) flap conformation. Simulations of inhibitor-bound PM II were carried out using the structure of the protein with the rs370 transition state analogue (PDB:1LF2 [21]). The aniline nitrogen ($pK_a = 4.87$ [22]) of the inhibitor was protonated, to mimic acidic conditions. Standard OPLS atom and bond types were used for the inhibitor. The atomic charges were set by fitting to the electrostatic potential around the molecule using the Kollman–Sing method [23], where the energy was calculated using Hartree–Fock self consistent field and the 6-31Gd Gaussian. Quantum chemical calculations were performed by the computer program GAMESS [24]. Although fast rotations were observed around the χ_2 dihedral angle of the catalytic aspartates in the simulations of the uncomplexed protein, the four possible locations of the proton (i.e., Oδ1 and Oδ2 of D34 and D214) were included in the simulations of the bound protein. All structures were downloaded from the protein data bank [25].

After the preparation of the protein structure, the protein was immersed in a truncated octahedral box containing TIP4P model waters [26]. Water molecules were removed from the box if the distance between any protein atom and any atom of the water was less than the sum of the van der Waals radii of both atoms. The edges of the box extended to at least 1.3 nm from the solute. Na^+ and Cl^- ions were added randomly by replacing non-crystallographic water molecules in order to neutralise the charge of the system and maintain a salt concentration of 0.1 M. Cation parameters derived by Åqvist were used for the sodium [27]. Before each MD simulation, internal constraints were relaxed by energy minimisation, until the maximal force on individual atoms was smaller than 100 kJ mol^{-1} nm^{-1}. After the minimisation, initial atomic velocities, corresponding to the Boltzmann distribution at a temperature of 300 K, were randomly assigned and a constrained MD run was performed for 100 ps. During the constrained simulations, protein heavy atoms were fixed to their initial positions with a force constant of 1000 kJ mol^{-1} nm^{-2}. The constraints were released, and the system was equilibrated for 1ns before data collection for analysis. During the MD runs, the LINCS algorithm [28] was used to constrain the lengths of bonds, while water molecules were kept rigid by use of the SETTLE algorithm [29]. The time step for the simulations was 2 fs. The temperature and pressure were coupled to an external bath with Berendsen's coupling algorithm [30] ($P_{ref} = 1$ bar, $\tau_P = 0.5$ ps; $T_{ref} = 300$ K; $\tau_T = 0.1$ ps). Van der Waals forces were truncated at 1.0 nm with a plain cutoff. Long-range electrostatic forces were treated using the particle mesh Ewald method [31]. A total of 22 simulations were performed, as summarised in Table 1. Root mean square deviation (RMSD) values, calculated over all heavy atoms in the backbone,are also reported in the table.

Table 1
Simulations details

Simulation[a]	PDB code	Protonated Asp	Duration (ns)	Maximal backbone RMSD (nm)
Mature 1	1LF4	214	20	0.23
Mature 2	1LF4	214	20	0.25
Mature 3	1LF4	34	20	0.27
Mature 4	1LF4	34	20	0.24
Alt. Flap 1	2BJU	214	20	0.28
Alt. Flap 2	2BJU	214	20	0.23
Alt. Flap 3	2BJU	214	20	0.27
Alt. Flap 4	2BJU	214	20	0.27
Cleaved 1	1PFZ	214	20	0.24
Cleaved 2	1PFZ	214	88	0.25
Cleaved 3	1PFZ	214	20	0.27
Cleaved 4	1PFZ	34	36	0.28
Cleaved 5	1PFZ	34	20	0.22
Cleaved 6	1PFZ	34	10	0.31
Complexed 1[b]	1LF2	214	20	0.22
Complexed 2[b]	1LF2	214	20	0.28
Complexed 3[b]	1LF2	214	10	0.21
Complexed 4[b]	1LF2	214	10	0.16
Complexed 5[b]	1LF2	34	10	0.17
Complexed 6[b]	1LF2	34	10	0.17
Complexed 7[b]	1LF2	34	10	0.15
Complexed 8[b]	1LF2	34	10	0.17

[a]Similar runs (e.g. mature 1 and mature 2) were started using different random distributions of the initial velocities.
[b]In the runs of the complex with the hydroxypropylamine inhibitor rs370 (Complexed), each catalytic aspartate was protonated twice on Oδ1 and twice on Oδ2.

2.2. Hydrogen bond analysis

Direct hydrogen bonds (HBs) between two residues were calculated with the program g_hbond, which is available in Gromacs. The criteria for a HB were a donor (nitrogen or oxygen) to acceptor (oxygen) distance $\leqslant$0.35 nm and an acceptor–donor–hydrogen angle $\leqslant$30°, i.e., default Gromacs parameters.

HBs between the Oδ atoms of the catalytic aspartates were also considered where the donor and acceptor were bridged by one water molecule. In this case, a HB was determined based only on a distance criterion, i.e., donor to water–oxygen and water–oxygen to acceptor distances $\leqslant$0.35 nm.

3. Results and discussion

3.1. Hydrogen bonds between the catalytic aspartates in the Apo enzyme

Analysis of direct and water-mediated HBs in the catalytic dyad is useful for assessing the structural stability of the active site. This analysis reveals that when D214 was protonated a HB between the catalytic aspartates was present during more than half of the simulation time in the runs of mature PM II (Table 2). On the other hand, when D34 was protonated, a direct HB between the carboxy groups of the catalytic aspartates was never observed and the formation of a solvent-mediated HB was sporadic. Furthermore, the simulations of cleaved proPM revealed a similar trend (Table 2). When D214 was protonated, direct HBs are rare but solvent-mediated HBs occur in about 18% of the simulation time. Conversely, the formation of HBs between the catalytic aspartates in the corresponding simulations with D34 protonated is infrequent (4% over all simulations).

A HB between the catalytic aspartates is not necessarily present when PM II is engaged in the catalytic activity or when it binds an inhibitor. Yet, in both cases the catalytic aspartates are located in the proximity of each other. The distributions of the closest Oδ–Oδ distances between D34 and D214 (Fig. 1) provide further evidence on the preferred protonation state. The distribution in the simulations of mature PM II with D214 protonated has two maxima, at 0.25 nm and 0.42–0.45 nm (Fig. 1, black trace). These maxima correspond to the location of the catalytic dyad either at a contact distance or separated by one water molecule. As a basis of comparison, the distance between the two nearest Oδs in the crystal structures is 0.27–0.35 nm (Fig. 1, shaded area) [15]. It should be noted that the distribution of distances observed in the simulations is not expected to fully overlap with the experimental values, which were determined in a non-physiological solution

Table 2
Percentage of HB presence in the simulations

Conformation	Protonation	D34–D214[a]		D34–S37[b]	S37–W41	W41–Y77	D214–T217[c]
		Direct	Total				
Mature	214	30	63	94	0	79	68
Mature	34	0	3	6	0	89	90
Alt. Flap	214	46	78	97	0	0	44
Cleaved	214	0	18	86	9	9	37
Cleaved	34	0	4	6	48	0	96
Complexed	214	83	92	100	0	86	77
Complexed	34	43	51	89	0	65	95

Percentage values were calculated upon cumulating simulations of the same type. For simulation conditions, see Table 1. The HBs were calculated only between the side-chain atoms.
[a]The total number of HBs includes solvent insertion.
[b]The hydroxyl of S37 acts as a donor.
[c]The hydroxyl of T217 acts as a donor.

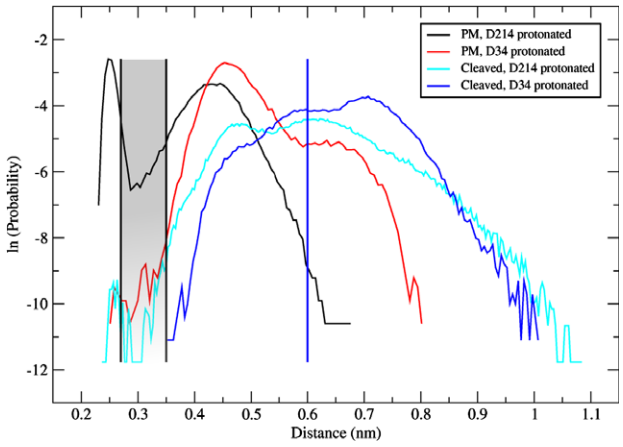

Fig. 1. The distributions of the minimal D34Oδ–D214Oδ distance. Black and red traces correspond to the simulations of the mature enzyme, cyan and blue traces to the simulations of the cleaved proenzyme. The vertical lines represent the distances in the crystal structures of PM II (shaded area) and proPM (blue). The corresponding distributions from the simulations of the complexed enzyme are similar to those of the apo-enzyme with D214 protonated, and are omitted from the figure for clarity.

that favours crystallisation. Yet, it is striking that the range of values observed in the crystal structures of PM II is much shorter than the distance distribution of the simulations with protonated D34 (Fig. 1, red trace).

The distributions of the closest Oδ–Oδ distances at the catalytic dyad in the simulations of the cleaved proPM are shifted to larger separation with respect to those of the mature enzyme. This difference is consistent with the crystal structures, as the corresponding distance is larger in proPM compared to mature PM II (0.60 versus 0.35 nm) [9,15]. Interestingly, the distance distribution in the simulation of the cleaved proPM with D214 protonated (cyan trace) has local maxima at 0.25 and 0.45 nm, which match a direct and a solvent-mediated HB, respectively. Note that the corresponding distribution for proPM with D34 protonated (blue trace) only starts at a distance of 0.35 nm. The protonation of D214 is therefore more likely to promote the activation of PM II.

3.2. The hydrogen bond network in the Apo active site

The catalytic site of PM II is characterised by a linear chain of HBs, reaching from the catalytic dyad to the flap region (T217–D214–water1–D34–S37–water2–Y77–W41) [15], as in most other pepsin-like enzymes of known three-dimensional structures [32]. Indeed, each of these HBs was present in more than 50% of the simulation time in the simulations of the mature PM II with D214 protonated.

Further analysis of the linear chain of HBs reveals that the protonation state of the catalytic aspartates has a strong influence on the presence or absence of these HBs. As an example, consider the S37Oγ–D34Oδ HB (where S37 is the donor), which is present in the crystal structure of apo PM II. This HB exists during 94% of the simulation time when D214 is protonated, but only during 6% of the time when D34 is protonated (Table 2). On the other hand, the T217Oγ1–D214Oδ HB, which is also present in the crystal structure, is more prevalent when D34 is protonated (during 90% compared to 68% of the simulations with protonated D214). This is in agreement with MD simulations of BACE, with protonated D32 (corresponding to D34 in PM II), during which the T231Oγ1–D228Oδ (T217 and D214 in PM) HB was stable [33]. However, in the simulations of BACE the S35Oγ–D32Oδ HB was not stable. Furthermore, while in the simulations of PM II water 2 is always a HB donor to S37, in BACE water2 and S35 switched their donor/acceptor roles when the S35Oγ–D32Oδ HB was broken, which, as the authors discussed, conforms with the catalytic mechanism suggested by Andreeva and Rumsh (based on the assumption that D32 is protonated) [32]. In PM II, water 2 is always a HB donor to S37 (Fig. 2), and when D34 is protonated the distance between D34 and D214 is too large to support the base activation catalytic mechanism. Interestingly, when D214 is protonated, the linear HB chain is similar to the HB arrangement which was suggested to stabilise the tetrahedral intermediate in pepsin-like proteases [32], even if the HB between W41 and Y77 is missing (Fig. 2A and C).

3.3. Simulations of the complexed enzyme

The rs370 transition state analog inhibitor (see Supplementary Fig. 1), has a hydroxypropylamine linker connecting Phe and Leu side chains in the P_1 and P_1' positions, respectively, mimicking the Phe-Leu scissile bond in haemoglobin. During the simulations, the inhibitor's hydroxyl group is involved as a donor in a hydrogen bond with one of the carboxylic oxygens of the charged residue (D34 when D214 is protonated and vice versa). This hydrogen bond is present in 98% of the simulation time when D214 is protonated, but only in 68% of the simulation time when D34 is protonated

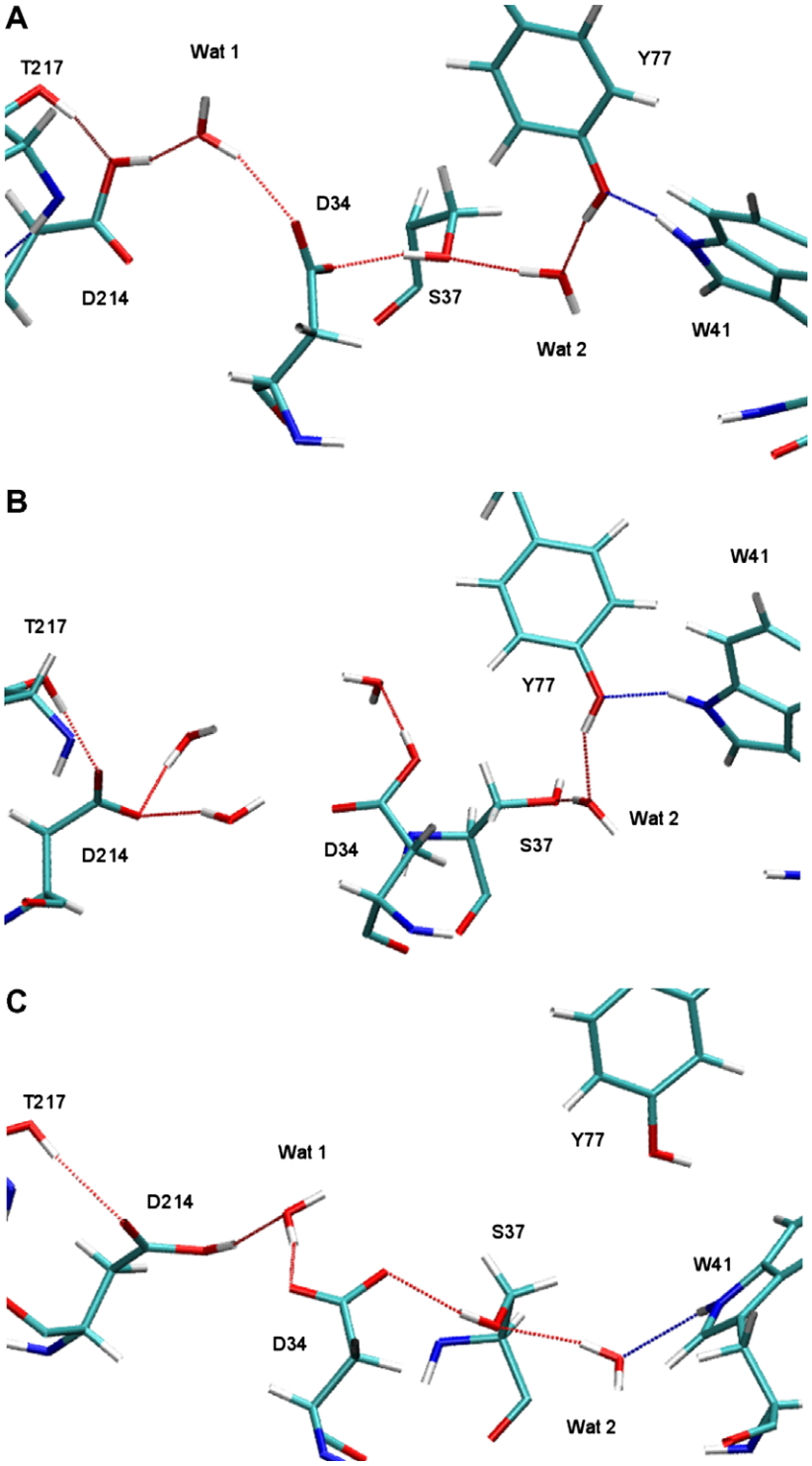

Fig. 2. The linear chain of HB in the substrate binding site in the simulations with (A) D214 protonated (the linear HB chain consists of T217–D214–water1–D34–S37–water2–Y77–W41); (B) D34 protonated (T217–D214, S37–water2–Y77–W41), and (C) D214 protonated and alternative flap conformation (T217–D214–water1–D34–S37–water2–W41).

(Table 3). The protonated aspartic acid donates a hydrogen either to the other catalytic residue or to the inhibitor's hydroxyl oxygen, and the linear chain of hydrogen bonds in the active site is almost always present in the simulations (Table 2). The stability of this linear chain of hydrogen bonds is higher when D214 is protonated. Moreover, in one of the four simulations with D34 protonated, the inhibitor started to exit from the active site after 4.4 ns of simulation time (see Supplementary Fig. 2). Conversely, the inhibitor was tightly bound to the enzyme in all four runs with protonated D214.

Table 3
Percentage of HB presence between the catalytic aspartates and the inhibitor

Donor	Acceptor	HB presence (%)	
		D214 protonated	D34 protonated
D214	Inhibitor	14	–
Inhibitor	D214	0	68
D34	Inhibitor	–	40
Inhibitor	D34	98	3

4. Conclusions

Multiple explicit-water MD simulations of PM II were performed to investigate the protonation state of the catalytic aspartates. To mimic the conditions before and during the process of substrate binding, PM II was simulated both uncomplexed (starting with different conformations of the flap) and in the complex with a transition state analogue inhibitor. The simulations' results and in particular the HB analysis and the distributions of minimal distance between Oδs show that protonation of D214 is more consistent with the crystallographic data and catalytic mechanism.

Acknowledgements: We thank Dr. A. Abebe Gorfe for critically reading of the manuscript. R.F. acknowledges the support from the Rothschild Foundation and the Forschungskredit Program of the University of Zürich.

Appendix A. Supplementary material

Supplementary data associated with this article can be found, in the online version, at doi:10.1016/j.febslet.2007.07.033.

References

[1] Ersmark, K., Samuelsson, B. and Hallberg, A. (2006) Plasmepsins as potential targets for new antimalarial therapy. Med. Res. Rev. 26, 626–666.
[2] Bjelic, S. and Åqvist, J. (2004) Computational prediction of structure, substrate binding mode, mechanism, and rate for a malaria protease with a novel type of active site. Biochemistry 43, 14521–14528.
[3] Bjelic, S. and Åqvist, J. (2006) Catalysis and linear free energy relationships in aspartic proteases. Biochemistry 45, 7709–7723.
[4] Carlsson, J., Ander, M., Nervall, M. and Åqvist, J. (2006) Continuum solvation models in the linear interaction energy method. J. Phys. Chem. B 110, 12034–12041.
[5] Bjelic, S., Nervall, M., Gutierrez-de Teran, H., Ersmark, K., Hallberg, A. and Åqvist, J. (2007) Computational inhibitor design against malaria plasmepsins. Cell Mol. Life Sci., in press. doi:10.1007/s00018-007-7102-2.
[6] McCarrick, M.A. and Kollman, P. (1994) Use of molecular dynamics and free energy perturbation calculations in anti-human immunodeficiency virus drug design. Methods Enzymol. 241, 370–384.
[7] Levy, Y., Caflisch, A., Onuchic, J.N. and Wolynes, P.G. (2004) The folding and dimerization of hiv-1 protease: evidence for a stable monomer from simulations. J. Mol. Biol. 340, 67–79.
[8] Chang, C.E., Trylska, J., Tozzini, V. and McCammon, J.A. (2007) Binding pathways of ligand to HIV-1 protease: coarse-grained and atomistic simulations. Chem. Biol. Drug Des. 69, 5–13.
[9] Khazanovich Bernstein, N., Cherney, M.M., Loetscher, H., Ridley, R.G. and James, M.N. (1999) Crystal structure of the novel aspartic proteinase zymogen proplasmepsin II from *Plasmodium falciparum*. Nat. Struct. Biol. 6, 32–37.
[10] Park, H. and Lee, S. (2003) Determination of the active site protonation state of beta-secretase from molecular dynamics simulation and docking experiment: implications for structure-based inhibitor design. J. Am. Chem. Soc. 125, 16416–16422.
[11] Rajamani, R. and Reynolds, C.H. (2004) Modeling the protonation states of the catalytic aspartates in beta-secretase. J. Med. Chem. 47, 5159–5166.
[12] Polgar, T. and Keseru, G.M. (2005) Virtual screening for beta-secretase (BACE1) inhibitors reveals the importance of protonation states at Asp32 and Asp228. J. Med. Chem. 48, 3749–3755.
[13] Yu, N., Hayik, S.A., Wang, B., Liao, N., Reynolds, C.H. and Merz, K.M. (2006) Assigning the protonation states of the key aspartates in beta-secretase using QM/MM X-ray structure refinement. J. Chem. Theory Comput. 2, 1057–1069.
[14] Gutierrez-de Teran, H., Nervall, M., Dunn, B.M., Clemente, J.C. and Åqvist, J. (2006) Computational analysis of plasmepsin IV bound to an allophenyl norstatine inhibitor. FEBS Lett. 580, 5910–5916.
[15] Asojo, O.A., Gulnik, S.V., Afonina, E., Yu, B., Ellman, J.A., Haque, T.S. and Silva, A.M. (2003) Novel uncomplexed and complexed structures of plasmepsin II, an aspartic protease from *Plasmodium falciparum*. J. Mol. Biol. 327, 173–181.
[16] Prade, L., Jones, A.F., Boss, C., Richard-Bildstein, S., Meyer, S., Binkert, C. and Bur, D. (2005) X-ray structure of plasmepsin II complexed with a potent achiral inhibitor. J. Biol. Chem. 280, 23837–23843.
[17] Berendsen, H.J.C., van der Spoel, D. and Vandrunen, R. (1995) Gromacs – a message-passing parallel molecular-dynamics implementation. Comput. Phys. Commun. 91, 43–56.
[18] van der Spoel, D., Lindahl, E., Hess, B., Groenhof, G., Mark, A.E. and Berendsen, H.J.C. (2005) Gromacs: fast, flexible, and free. J. Comput. Chem. 26, 1701–1718.
[19] Jorgensen, W.L., Maxwell, D.S. and Tirado-Rives, J. (1996) Development and testing of the opls all-atom force field on conformational energetics and properties of organic liquids. J. Am. Chem. Soc. 118, 11225–11236.
[20] Khazanovich Bernstein, N., Cherney, M.M., Yowell, C.A., Dame, J.B. and James, M.N. (2003) Structural insights into the activation of *P. vivax* plasmepsin. J. Mol. Biol. 329, 505–524.
[21] Asojo, O.A., Afotina, A., Gulnik, S.V., Yu, B., Erickson, J.W., Randad, R., Medjahed, D. and Silva, A.M. (2002) Structures of Ser205 mutant plasmepsin II from *Plasmodium falciparum* at 1.8 angstrom in complex with the inhibitors rs367 and rs370. Acta Crystallogr. D 58, 2001–2008.
[22] Albert, A. and Serjeant, E.P. (1984) The Determination of Ionization Constants: A Laboratory Manual, 3rd ed, Chapman and Hall.
[23] Singh, U.C. and Kollman, P.A. (1984) An approach to computing electrostatic charges for molecules. J. Comp. Chem. 5, 129–145.
[24] Schmidt, M.W. et al. (1993) General atomic and molecular electronic structure system. J. Comput. Chem. 14, 1347–1363.
[25] Berman, H.M., Westbrook, J., Feng, Z., Gilliland, G., Bhat, T.N., Weissig, H., Shindyalov, I.N. and Bourne, P.E. (2000) The protein data bank. Nucleic Acids Res. 28, 235–242.
[26] Jorgensen, W.L., Chandrasekhar, J., Madura, J.D., Impey, R.W. and Klein, M.L. (1983) Comparison of simple potential functions for simulating liquid water. J. Chem. Phys. 79, 926–935.
[27] Åqvist, J. (1990) Ion–water interaction potentials derived from free energy perturbation simulations. J. Chem. Phys. 94, 8021–8024.
[28] Hess, B., Bekker, H., Berendsen, H.J.C. and Fraaije, J.G.E.M. (1997) Lincs: A linear constraint solver for molecular simulations. J. Comp. Chem. 18, 1463–1472.
[29] Miyamoto, S. and Kollman, P.A. (1992) Settle: an analytical version of the shake and rattle algorithms for rigid water models. J. Comp. Chem. 13, 952–962.
[30] Berendsen, H.J.C., Postma, J.P.M., DiNola, A. and Haak, J.R. (1984) Molecular dynamics with coupling to an external bath. J. Chem. Phys. 81, 3684–3690.
[31] Darden, T., York, D. and Pedersen, L. (1993) Particle mesh ewald: An *n*-log(*n*) method for ewald sums in large systems. J. Chem. Phys. 98, 10089–10092.
[32] Andreeva, N.S. and Rumsh, L.D. (2001) Analysis of crystal structures of aspartic proteinases: on the role of amino acid residues adjacent to the catalytic site of pepsin-like enzymes. Protein Sci. 10, 2439–2450.
[33] Gorfe, A.A. and Caflisch, A. (2005) Functional plasticity in the substrate binding site of beta-secretase. Structure 13, 1487–1498.